

IDENTIFICATION AND MITIGATION OF SMOKE-RING EFFECTS IN SCINTILLATOR-BASED ELECTRON BEAM IMAGES AT THE EUROPEAN XFEL

G. Kube, A. Novokshonov, S. Liu, M. Scholz, DESY, Hamburg, Germany

Abstract

Standard transverse beam profile measurements at the European XFEL are based on scintillating screen monitors using LYSO:Ce as scintillator material. While it is possible to resolve beam sizes down to a few micrometers with this material, the experience during the XFEL commissioning showed that the measured emittance values were significantly larger than the expected ones. In addition, beam profiles measured at bunch charges of a few hundred pC showed a 'smoke ring' structure. While coherent OTR emission and beam dynamical influence could be excluded, it is assumed that the profile distortions are caused by effects from the scintillator material itself. Following the experience in high energy physics, a simple model was developed which takes into account quenching effects of excitonic carriers inside the scintillator in a heuristic way. Based on this model, the observed beam profiles can be understood qualitatively. Possible new scintillator materials suitable for beam profile diagnostics are discussed and preliminary test results from beam measurements at the European XFEL are presented.

INTRODUCTION

Transverse beam profile diagnostics in electron linacs is widely based on optical transition radiation (OTR) as standard technique which is observed in backward direction when a charged particle beam crosses the boundary between two media with different dielectric properties. Unfortunately, microbunching instabilities in high-brightness electron beams of modern linac-driven free-electron lasers (FELs) can lead to coherence effects in the emission of OTR, thus rendering it impossible to obtain a direct image of the particle beam and compromising the use of OTR monitors as reliable diagnostics for transverse beam profiles. The observation of coherent OTR (COTR) has been reported by several facilities (see e.g. Ref. [1]), and in the meantime the effect of the microbunching instability is well understood [2].

For the European XFEL it was therefore decided to use scintillation screen monitors because the light emission in a scintillator is a multistage stochastic process from many atoms which is completely insensitive to the longitudinal bunch structure. In a series of test measurements performed in the past few years, the applicability of inorganic scintillators for high resolution electron beam profile measurements was investigated [3, 4]. Most notably, the dependency of the resolution on the scintillator material and on the observation geometry was studied with respect to resolve beam profiles in the order of several tens of micrometers, and it was concluded that LYSO ($\text{Lu}_{2(1-x)}\text{Y}_{2x}\text{SiO}_5:\text{Ce}$) is a suitable material because it gives the best spatial resolution.

Based on these measurements, screen monitor stations were designed for the European XFEL using 200 μm thick LYSO screens [5]. In a high resolution beam profile measurement using an XFEL-type screen it was demonstrated that it is possible to resolve a vertical beam size of $\sigma_y = 1.44 \mu\text{m}$ [6].

However, the experience during the commissioning of the XFEL showed that the measured emittance values were significantly larger than the expected ones [7, 8]. In addition, beam profiles measured at bunch charges of a few hundreds of pico-Coulomb show a 'smoke ring' shaped structure, see e.g. Fig. 1.

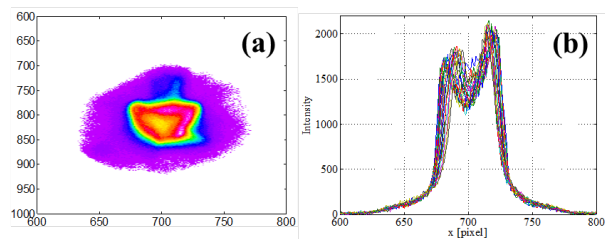


Figure 1: (a) Typical smoke ring shaped beam profile as measured with an XFEL screen monitor based on a 200 μm thick LYSO screen. (b) Various horizontal cuts through the 2D-profile demonstrate the intensity drop in the central part of the beam spot.

While the contribution of COTR emission from the scintillator surface, beam dynamical influence, and camera effects could be excluded to explain this observation, it is assumed that the beam profile distortions are caused by effects from the scintillator material.

In Ref. [9], a simple model was presented which takes into account quenching effects of excitonic carriers inside a scintillator in a heuristic way. Based on this model, the observed beam profiles could be understood qualitatively. In the following, the underlying ideas are briefly summarized with the emphasis on first results from beam measurements at the European XFEL with new scintillator materials suitable for beam profile diagnostics.

SCINTILLATOR MODEL

Degradation effects in scintillator based beam profile measurements are reported in a number of publications, see e.g. Refs. [10–15]. The scintillator influence is mainly interpreted as saturation of the measured profiles, caused e.g. by full excitation of the luminescent centers in some regions inside the scintillator. While inspecting Fig. 1 it is obvious that the XFEL observations cannot simply be described by a saturation effect which would result in a flattening of the

Content from this work may be used under the terms of the CC BY 3.0 licence © (2019). Any distribution of this work must maintain attribution to the author(s), title of the work, publisher, and DOI

measured beam profiles. It rather leads to the conclusion that luminescent centers may even be quenched in the central part of the beam spot such that the scintillating light intensity is decreased in these regions.

Taking into account the experience of high energy physics, it is known that scintillator based electron calorimeters possess a non-linear energy resolution, and the degree of non-linearity depends on the scintillator material. Following the explanations e.g. in Ref. [16] this effect can be attributed to the ionization density inside the material: if the density is above a critical limit, excitonic states can annihilate in an Auger-like process without creating a scintillating photon. In case of calorimetry the critical ionization density occurs at the end of a particle shower where the particle energy loss is dominated by the kinematical factor β^{-2} ($\beta = v/c$) according to the Bethe–Bloch equation. As a result, the relative light yield in a scintillator typically decreases with decreasing electron energy, see e.g. Ref. [17] and the figures therein. Following Refs. [16, 18], an improvement of the scintillator linearity should in principle correlate with the minimization of the interaction time of excitonic states (electron/hole pairs, excitons, ...) with surrounding traps such that their energy transfer to luminescent centers is unperturbed.

Translating this principle to the case of beam profile diagnostics of ultra-relativistic electron beams, the main idea is that the ionization track density which is responsible for the non-linear scintillator behavior is determined by the primary beam particle density rather than by the secondary energy of shower particles. Following Ref. [9] the ionization tracks inside a scintillator can be modeled as straight tubes, homogeneously filled with electrons and holes. The tube radius is estimated by the Fermi radius $R_S \approx c/\omega_p$ with ω_p the plasma frequency of the material. While dynamical processes in scintillators take place in the order of 10^{-12} – 10^{-10} s, the charges inside the ionization tubes can be considered as static with respect to the particle beam dynamics. The situation is schematically depicted in Fig. 2 for the case of a beam with low and with high particle density. Due to the static behavior of the ionization tubes, for the description of the ionization track density a two-dimensional representation

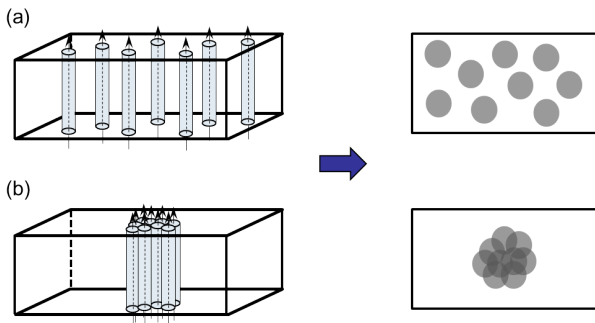


Figure 2: Passage of individual electrons through a scintillator in the case of (a) low and (b) high particle density. Each electron creates a homogeneous ionization tube. Due to the static behavior of the ionization tubes a two-dimensional representation is sufficient.

tion is sufficient as shown on the right side of this figure. In order to estimate particle track densities in cases of a beam with high particle density, a simple geometrical model is used in which the density is estimated as the sum of tube area and track intersections.

Based on these illustrative assumptions, distorted beam profiles are calculated in four consecutive steps. In the first step, the transverse particle beam profile (which is assumed to be Gaussian in the following) is transformed into a 2D surface density profile describing the local particle density. In the second step, the mean distance between the ionization tubes is calculated considering the nearest neighbor distribution. With knowledge of the mean distance, afterwards a regular grid of neighboring tubes is constructed and the density of the local tracks $n_i(x, y)$ is geometrically estimated as described above. Finally, for each point of the beam profile a weighting factor $w(x, y)$ is calculated

$$w(x, y) = \frac{1}{1 + \alpha \frac{dE}{dx}(x, y)}$$

which is similar to the formula of Birks [19] describing the non-linearity in the scintillator light yield. Here it is assumed that $\frac{dE}{dx} \propto n_i^3$ and α is a freely adjustable parameter describing the quenching strength.

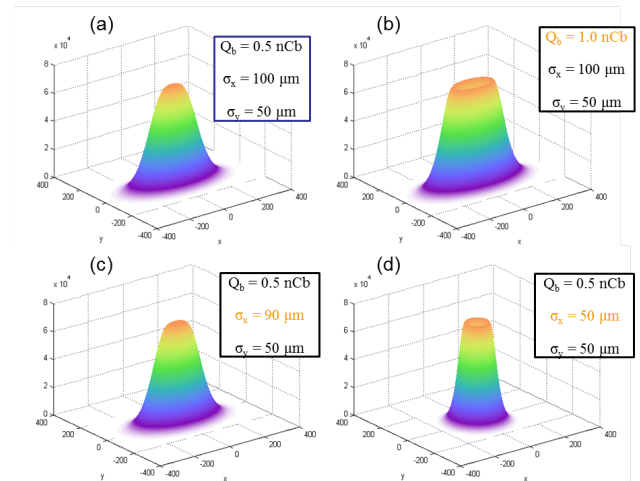


Figure 3: Calculated beam profiles according to the model described in this work. Starting with typical XFEL beam parameters (a) and assuming that $\alpha = 6.4 \times 10^{-5}$, beam profiles for increased bunch charge (b) or decreased horizontal beam size (c,d) are shown.

As an example, Fig. 3 shows calculated beam profiles according to the proposed model presented. Starting with a Gaussian beam profile and typical XFEL beam parameters (a) it can be seen that both increasing the bunch charge (b) and reducing the beam size (c,d) may result in a pronounced beam profile degradation which is caused by an increase in the local ionization track density in the central part of the beam interaction region with the scintillator. Thereby it is possible to produce smoke ring shaped beam profiles as observed at the XFEL.

MITIGATION AND FIRST TEST EXPERIMENTS

Based on to the model described in detail in Ref. [9] and summarized in the previous section, smoke ring shaped beam profiles as observed at the European XFEL can be reproduced. The model takes into account quenching effects of excitonic carriers inside a scintillator in a heuristic way, the level of quenching in the central part of the beam generated spot depends on bunch charge and beam size, i.e. it is controlled by the particle density. However, the model provides no information about suitable scintillator materials for beam profile diagnostic applications because the quenching strength α introduced before is a freely adjustable parameter without direct connection to accessible material properties.

In this context it helps again to refer to the experience of the scintillator community for high energy physics. As shown in Ref. [17], "silicate" based scintillators as LSO, YSO, LPS where the oxygen is intimately bound to the silicon as a SiO_4^{4-} moiety exhibit a strong non-linear behavior, the same holds for LYSO which has similar properties than LSO. In the same reference it is pointed out that exciton-exciton quenching in LuAG doped either with Ce or Pr should be small. However, the resolution study performed in Ref. [4] indicated that the spatial resolution of a LuAG scintillator was worse compared to a LYSO screen. Therefore other materials could be more promising. As previously mentioned, improving the linearity of a scintillator should in principle correlate with the minimization of the interaction time of excitonic states. In this context scintillator materials where gadolinium is stoichiometrically incorporated in the crystal structure seem to be promising [17]. In these materials it is assumed that excitation carriers can rapidly transfer their energy to excited states of gadolinium, and a rapid migration of this energy among the Gd sub-lattice is expected until a Ce doping ion is reached. According to Ref. [20] YAP could also be an interesting material because it exhibits a high mobility of excitonic carriers which may reduce the quenching probability.

In order to test scintillator materials for beam profile diagnostics under realistic conditions, a number of screen stations at the European XFEL was equipped with a LYSO screen together with an additional screen material. Three different materials were selected for first tests, YAG (yttrium aluminium garnet, $\text{Y}_3\text{Al}_5\text{O}_{12}:\text{Ce}$), YAP (yttrium aluminium perovskite, $\text{YAlO}_3:\text{Ce}$), and GAGG (gadolinium aluminium gallium garnet, $\text{Gd}_3\text{Al}_2\text{Ga}_3\text{O}_{12}:\text{Ce}$). While YAG is a material which is widely in use in particle beam diagnostics, YAP has a high mobility of excitonic carriers, and GAGG

Table 1: Scintillating Screen Materials under Test

material	yield [ph/keV]	λ_{max} [nm]	ρ [g/cm ³]
YAG	15 - 35	550	4.53
YAP	25	370	5.37
GGAG	50	530	6.7
LYSO	24	420	7.1

is a material containing Gd, thus the latter two materials are of potential interest in view of linearity. In Table 1 the main parameters light yield, maximum emission wavelength λ_{max} , and density ρ for the materials under test are summarized. While YAG emits light in the soft ultraviolet which is not well fitted to the sensitivity of a camera chip, GAGG is a new non-hygroscopic scintillator material on the market with high light yield and well matched to the camera chip sensitivity, thus attracting special attention for various applications.

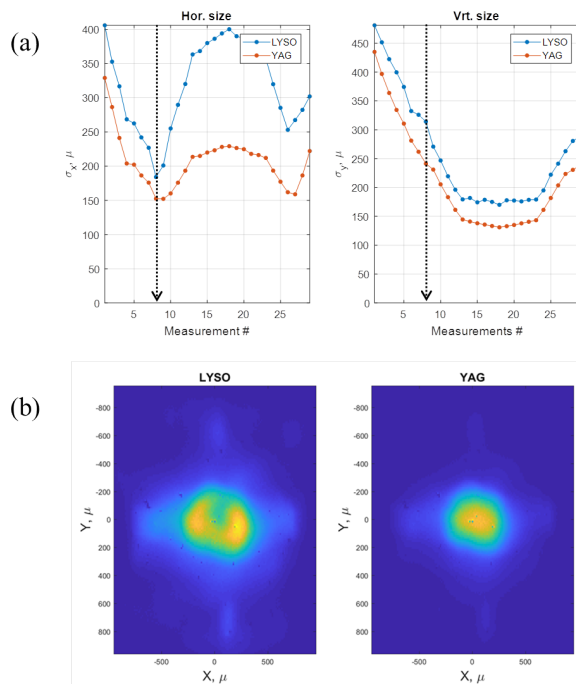


Figure 4: (a) Comparative resolution study using a YAG and a LYSO scintillator at the XFEL. The arrows indicate that measurement where the LYSO beam spot shows the transition to the smoke ring structure. (b) Corresponding beam images at the transition point.

In a first test experiment, profile measurements from a YAG and a LYSO screen were compared for identical beam and camera parameters. Both screens are mounted in the same screen station, and beam images were recorded for individual bunches with charge $Q_b \approx 1$ nC at a beam energy of about 14 GeV. In Fig. 4(a) a series of measurements is shown which was taken while the beam sizes were focused down, thus increasing the ionization track density in the central part of the beam interaction region with the scintillator. As can be seen, the LYSO-based beam size measurements are systematically larger than the ones with the YAG screen. Furthermore, starting from a certain particle density threshold the LYSO measurements show a clear signature of a smoke ring while the YAG measurement is unaffected, c.f. Fig. 4(b).

Keeping in mind that the occurrence of the smoke ring structure is connected with quenching of excitation carriers and causes a decrease of the scintillator light output, it is

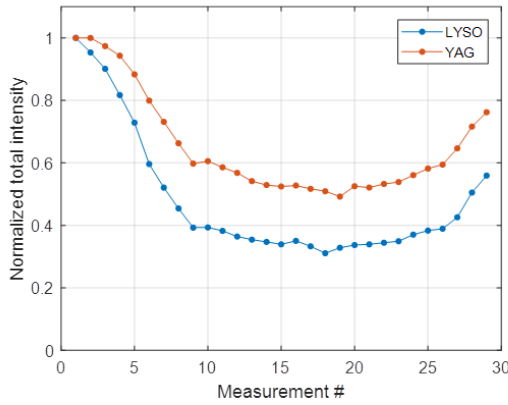


Figure 5: Normalized intensities for the comparative LYSO/YAG measurement series plotted in Fig. 4. The intensity drop is an indication for the onset of scintillator non-linearities.

illustrative to plot this light yield for the individual measurements as shown in Fig. 5. For better comparison, intensities are normalized to the one of the first measurement where no influence of a smoke ring structure is visible. As can be seen from this figure, the light yield of both screens is decreased while focusing the beam, thus indicating that in principle both screen materials are affected by non-linearities. In the case of LYSO this effect seems to be more distinct due to the visibility of the smoke ring structure.

The test experiment was repeated with another screen station where a YAP and a LYSO screen are installed together. While the beam energy was comparable to the previous measurement series, the bunch charge amounted to $Q_b \approx 0.45$ nC. However, as shown in Fig. 6 the beam spot could be focused down to much smaller sizes such that the maximum peak charge density which was roughly estimated

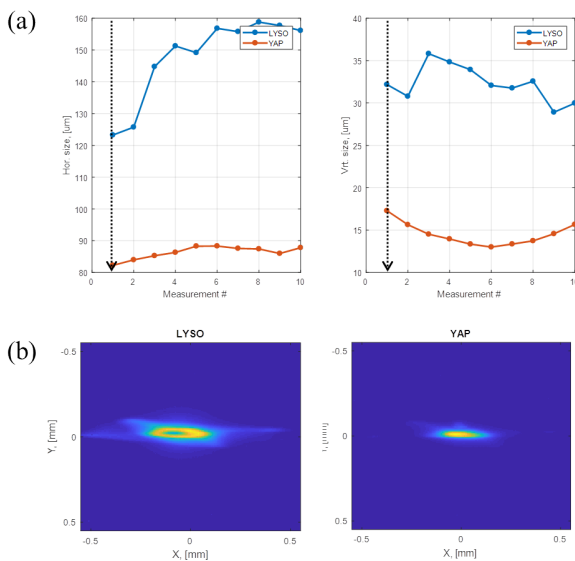


Figure 6: (a) Comparative resolution study using a YAP and a LYSO scintillator. The arrows indicate that measurement for which the beam images in (b) are plotted.

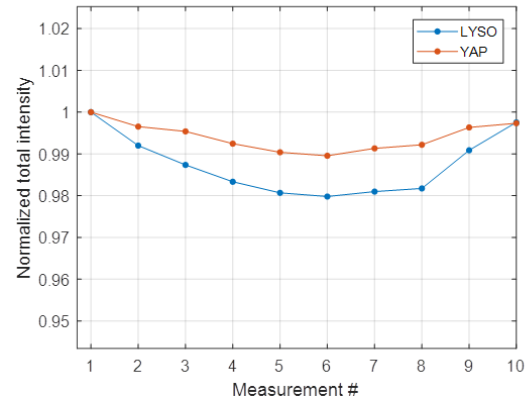


Figure 7: Normalized intensities for the comparative LYSO/YAP measurement series plotted in Fig. 6. The intensity drop for the LYSO screen is much smaller than in the previous measurement because all LYSO based profile measurements showed a smoke ring structure, thus the reference intensity is already affected by non-linearities.

to about $62 \text{ fC}/\mu\text{m}^2$ was significantly higher than in the previous experiment.

As can be seen from Fig. 6(a), the LYSO-based beam size measurements are again systematically larger than the ones with the YAP screen. In this experiment it was even not possible to increase the beam size to a level that no smoke ring structure was measured with the LYSO screen, already the first measurement is affected by this effect, c.f. the measured beam images in Fig. 6(b).

However, even for these large charge densities the YAP based beam images were undisturbed, as shown in Fig. 7 the drop in the normalized intensity is in the order of about 1% over the whole range of measurements.

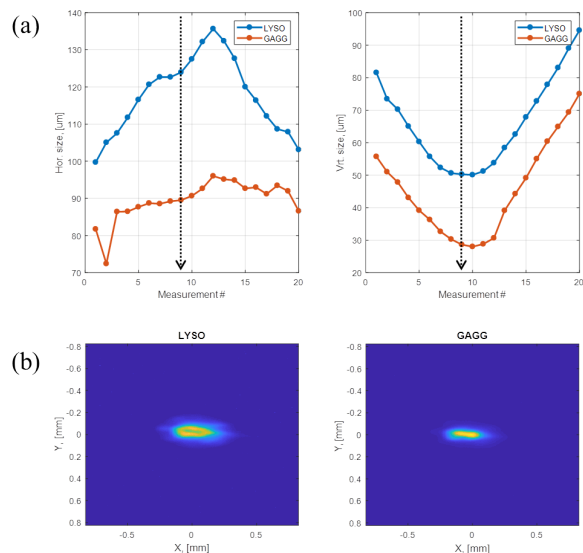


Figure 8: (a) Comparative resolution study using a GAGG and a LYSO scintillator. The arrows indicate that measurement where the LYSO beam spot shows the transition to the smoke ring structure. (b) Corresponding beam images at the transition point.

Content from this work may be used under the terms of the CC BY 3.0 licence (© 2019). Any distribution of this work must maintain attribution to the author(s), title of the work, publisher, and DOI

In the last test experiment, a GAGG screen was compared to LYSO, beam energy and bunch charge were the same Z for the previous YAP measurements. In this experiment, the achievable minimum beam size was slightly larger than before (c.f. Fig. 8(a)), the maximum peak charge density was roughly estimated to about $28 \text{ fC}/\mu\text{m}^2$. Again the LYSO-based beam size measurements are systematically larger than the ones with GAGG, and starting from a certain particle density threshold the LYSO measurements show a clear signature of a smoke ring structure while the GAGG measurements are unaffected, c.f. Fig. 8(b).

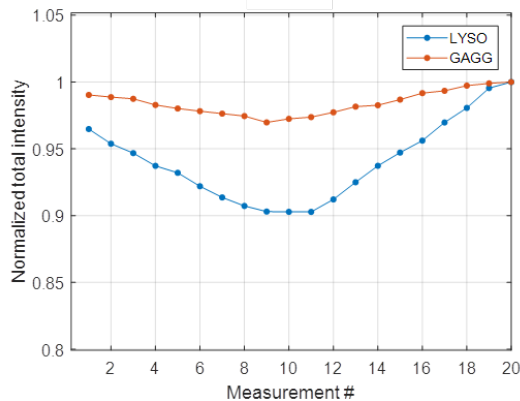


Figure 9: Normalized intensities for the comparative LYSO/GAGG measurement series plotted in Fig. 8.

This behaviour is reflected in the normalized intensity which is depicted in Fig. 9. In this case, the drop for GAGG is in the order of about 2% over the whole range of measurements while the one for LYSO amounts to about 10%.

Compared to the first test experiment with YAG, the drop of the normalized LYSO intensity is much smaller for the GAGG measurement. Presently it is not clear where the difference is coming from, this is a point for future investigations.

SUMMARY AND OUTLOOK

Based on the observation of smoke ring shaped beam profiles using screen monitor stations at the XFEL which utilize LYSO as standard scintillator material, a simple model is presented which takes into account quenching effects of excitonic carriers inside a scintillator in a heuristic way. With the help of this model, it is possible to reproduce smoke ring shaped beam profiles: the level of quenching in the central part of the beam generated spot in the scintillator depends on bunch charge and beam size, i.e. it is controlled by the particle density.

Improving the linearity of a scintillator should in principle correlate with the minimization of the interaction time of excitonic states. Based on the experience of high energy physics, gadolinium based scintillator materials like GAGG or YAP with its high mobility of the excitation carriers could in principle be interesting for future applications.

A series of test experiments was conducted at the European XFEL. In these experiments, beam images measured

with standard LYSO screens were compared to YAG and to YAP/ GAGG-based measurements. It could be demonstrated that LYSO as scintillator material shows strong non-linearities which render its application difficult in particle beam diagnostics. Even YAG which is widely used for beam profile measurements seems to show non-linear behaviour. However, smoke ring like structures could not be observed with this material. At the other hand, YAP and GAGG demonstrated to have a rather stable behaviour even at highest charge densities. Presently, more detailed studies are in preparation. Nevertheless it is planned already now to replace screens in the XFEL injector by GAGG as scintillator material.

REFERENCES

- [1] S. Wesch and B. Schmidt, “Summary of COTR Effects”, in *Proc. DIPAC’11*, Hamburg, Germany, May 2011, paper WEOA01, pp. 539–543.
- [2] G. V. Stupakov, “Control and Application of Beam Microbunching in High Brightness Linac-driven Free Electron Lasers”, in *Proc. IPAC’14*, Dresden, Germany, Jun. 2014, pp. 2789–2793. doi:10.18429/JACoW-IPAC2014-THYA01
- [3] G. Kube, C. Behrens, and W. Lauth, “Resolution Studies of Inorganic Scintillation Screens for High Energy and High Brilliance Electron Beams”, in *Proc. IPAC’10*, Kyoto, Japan, May 2010, paper MOPD088, pp. 906–908.
- [4] G. Kube, C. Behrens, C. Gerth, B. Schmidt, W. Lauth, and M. Yan, “Inorganic Scintillators for Particle Beam Profile Diagnostics of Highly Brilliant and Highly Energetic Electron Beams”, in *Proc. IPAC’12*, New Orleans, LA, USA, May 2012, paper WEOAA02, pp. 2119–2121.
- [5] Ch. Wiebers, M. Holz, G. Kube, D. Noelle, G. Priebe, and H.-Ch. Schroeder, “Scintillating Screen Monitors for Transverse Electron Beam Profile Diagnostics at the European XFEL”, in *Proc. IBIC’13*, Oxford, UK, Sep. 2013, paper WEPF03, pp. 807–810.
- [6] G. Kube *et al.*, “Transverse Beam Profile Imaging of Few-Micrometer Beam Sizes Based on a Scintillator Screen”, in *Proc. IBIC’15*, Melbourne, Australia, Sep. 2015, pp. 330–334. doi:10.18429/JACoW-IBIC2015-TUPB012
- [7] B. Beutner, “European XFEL Injector Commissioning Results”, in *Proc. FEL’17*, Santa Fe, NM, USA, Aug. 2017, pp. 389–393. doi:10.18429/JACoW-FEL2017-WEA01
- [8] D. Nölle, “The Diagnostic System at the European XFEL; Commissioning and First User Operation”, in *Proc. IBIC’18*, Shanghai, China, Sep. 2018, pp. 162–168. doi:10.18429/JACoW-IBIC2018-TUOA01
- [9] G. Kube, S. Liu, A. I. Novokshonov, and M. Scholz, “A Simple Model to Describe Smoke Ring Shaped Beam Profile Measurements With Scintillating Screens at the European XFEL”, in *Proc. IBIC’18*, Shanghai, China, Sep. 2018, pp. 366–370. doi:10.18429/JACoW-IBIC2018-WEOC03
- [10] A. Murokh, J. Rosenzweig, V. Yakimenko, E. Johnson, and X.J. Wang, “Limitations on the Resolution of Yag:Ce Beam Profile Monitor for High Brightness Electron Beam”, *The Physics of High Brightness Beams*, pp. 564–580, 2000. doi:10.1142/9789812792181_0038

Content from this work may be used under the terms of the CC BY 3.0 licence (© 2019). Any distribution of this work must maintain attribution to the author(s), title of the work, publisher, and DOI

- [11] A. Murokh, I. Ben-Zvi, J.B. Rosenzweig, X.J. Wang, and V. Yakimenko, "Limitations on Measuring a Transverse Profile of Ultra-Dense Electron Beams with Scintillators", in *Proc. PAC'01*, Chicago, IL, USA, Jun. 2001, paper TPAH049, p. 1333.
- [12] T. F. Silva, Z.O. Guimarães-Filho, C. Jahnke, and M.N. Martins, "Electron Beam Profile Determination: The Influence of Charge Saturation in Phosphor Screens", in *Proc. PAC'09*, Vancouver, Canada, May 2009, paper TH6REP040, pp. 4039–4041.
- [13] U. Iriso, G. Benedetti, and F. Pérez, "Experience with YAG and OTR Screens at ALBA", in *Proc. DIPAC'09*, Basel, Switzerland, May 2009, paper TUPB15, pp. 200–202.
- [14] F. Miyahara *et al.*, "Response of Scintillating Screens to High Charge Density Electron Beam", in *Proc. IPAC'17*, Copenhagen, Denmark, May 2017, paper MOPAB067, pp. 268–270. doi:10.18429/JACoW-IPAC2017-MOPAB067
- [15] R. Ischebeck *et al.*, "Characterization of High-Brightness Electron Beams at the Frontiers of Temporal and Spatial Resolution", presented at FEL2017, Santa Fe, NM, USA, Aug. 2017, paper WEB01, unpublished.
- [16] W. W. Moses *et al.*, "Scintillator Non-Proportionality: Present Understanding and Future Challenges", *IEEE Trans. Nucl. Sci.*, vol. 55, pp. 1049, 2008. doi:10.1109/tns.2008.922802
- [17] S. A. Payne *et al.*, "Nonproportionality of Scintillator Detectors: Theory and Experiment. II", *IEEE Trans. Nucl. Sci.*, vol. 58, pp. 3392, 2011. doi:10.1109/TNS.2011.2167687
- [18] A. N. Vasil'ev, in *Proc. SCINT'99*, Moscow, Russia, August 1999, p.43, 1999.
- [19] J. B. Birks, "Scintillations from Organic Crystals: Specific Fluorescence and Relative Response to Different Radiations", *Proc. Phys. Soc.*, vol. A64 pp. 874, 1951. doi:10.1088/0370-1298/64/10/303
- [20] Q. Li *et al.*, "A transport-based model of material trends in nonproportionality of scintillators", *J. Appl. Phys.*, vol. 109, pp. 123716, 2011. doi:10.1063/1.3600070